European Journal of Medicinal Chemistry 95 (2015) 369–376

Contents lists available at ScienceDirect

European Journal of Medicinal Chemistry

journal homepage: http://www.elsevier.com/locate/ejmech

Original article

Histone deacetylase inhibitor-polymer conjugate nanoparticles for acid-responsive drug delivery

Iza Denis [a, b, c], Fatima el Bahhaj [e], Floraine Collette [d], Régis Delatouche [e], Fabien Gueugnon [a, b, c], Daniel Pouliquen [a, b, c], Loic Pichavant [d], Valérie Héroguez [d, *], Marc Grégoire [a, b, c], Philippe Bertrand [e, *], Christophe Blanquart [a, b, c, *]

[a] Inserm, U892, Nantes F-44000, France
[b] CNRS, UMR 6299, Nantes F-44000, France
[c] University of Nantes, Nantes F-44000, France
[d] Laboratoire de Chimie des Polymères Organiques, CNRS, UMR 5629, Bordeaux, 16 Avenue Pey-Berland, F-33607 Pessac, France
[e] Institut de Chimie des Milieux et Matériaux de Poitiers, CNRS, UMR 7285, Poitiers. 4, Rue Michel Brunet, TSA 51106, B27 86073 Poitiers Cedex 9, France

ARTICLE INFO

Article history:
Received 19 January 2015
Received in revised form
13 March 2015
Accepted 17 March 2015
Available online 18 March 2015

Keywords:
Polymeric nanoparticle
Epigenetic inhibitor
Drug delivery
Controlled release
Stimuli-responsive

ABSTRACT

We report the synthesis of acid–responsive polymeric nanoparticles (NPs) consisting of a polymer-histone deacetylase inhibitor conjugate. An innovative aspect of this drug delivery particle lies in the NP conjugation of a histone deacetylase (HDAC) inhibitor, CI-994 (Tacedinaline), introduced with a clickable acid-responsive prodrug during monomer synthesis, prior to polymerization. Another novelty lies in the selected norbornene (NB)-polyethylene oxide (PEO) macromonomer allowing standardization of the polymerization process by Ring-Opening Metathesis Polymerization (ROMP) and functionalization through azide-alkyne click chemistry. Herein we demonstrate that the synthesized polymer gave 300 nm core–shell spherical nanoparticles with low dispersity (0.04), high water dispersability thanks to the PEO shell and well controlled HDAC inhibitor prodrug loading. Bioluminescence Resonance Energy Transfer (BRET) assay in living cells and viability experiments demonstrated efficient cellular internalization without additional chemistry, drug release inside cells with restoration of the HDAC inhibition and induction of apoptosis. Such NPs should minimize drug release *in vivo* during blood circulation and trigger intracellular delivery after endocytosis, holding promises for improved efficacy of this class of epigenetic inhibitors. This standardized synthesis paves the way for multifunctional nanoparticles synthesis.

1. Introduction

Epigenetic modifications, which are responsible for heritable changes of genes activity that are independent of changes in DNA sequence, are hallmark of several pathologies. All these modifications are used to fine-tune gene expression through changes in chromatin structure. Deregulation of these subtle mechanisms, leading to the abnormal expression of key regulatory genes, is implicated in various diseases including cancers [1]. These modifications called epigenetic marks consist in reversible chemical modifications on DNA and post-translational modifications (PTMs) of histones, mediated by the opposite actions of several protein families defined as epigenetic marks writers, erasers and readers and leading to the "histone code" [2]. DNA methylation is regulated by DNA methyl transferases (DNMT) and for demethylation by cytosine oxidases (TET) as well as base excision repair mechanisms. Histones can be acetylated or methylated via histone acetyl transferases (HAT) and deacetylases (HDAC) whose opposite activities equilibrate histone acetylation, and histone or protein arginine methyl transferases (HMT and PRMT) with the histone

Abbreviations: ADCA, adenocarcinoma; BrD, bromodomain; BRET, bioluminescence resonance energy transfer; DDS, drug delivery system; DLS, dynamic light scattering; DMF, dimethyl formamide; FITC, fluorescein-isothiocyanate; HDAC, histone deacetylases; HDACi, histone deacetylase inhibitor; mBu, milliBRET units; MPM, malignant pleural mesothelioma; NB, norbornene; NPs, nanoparticles; PDI, polydispersity index; PEO, polyethylene oxide; PMDETA, pentamethyldiethylenetriamine; PTM, post-translational modifications; ROMP, ring-opening metathesis polymerization; SEC, size exclusion chromatography; THF, tetrahydrofuran; TLC, thin layer chromatography; TSG, tumor suppressor genes.

* Corresponding authors. Institut de Chimie des Milieux et Matériaux Poitiers, France.
E-mail address: philippe.bertrand@univ-poitiers.fr (P. Bertrand).

http://dx.doi.org/10.1016/j.ejmech.2015.03.037
0223-5234/

demethylases counterparts (HDM) [3]. HDACs are one of the most studied epigenetic targets. Indeed, HDACs are overexpressed in numerous cancer cells, which leads to histone hypoacetylation involved in tumour suppressor genes (TSG) down regulation, like p21 [4]. Inhibitors of HDACs (HDACi) have been investigated in the past two decades as an alternative strategy to fight diseases resulting from the overexpression or modified activity of these epigenetic proteins. HDACi induce an increase of acetylated histones, which leads to chromatin relaxation along with an increase of gene transcription, notably TSG gene transcription [5]. In addition HDACi displayed interesting anti-tumor properties on a large number of different malignant cells [6]. These compounds are considered nowadays in clinic in single or combined therapies against various diseases like cancer [7] and in particular when current therapies failed [5,8]. However, HDACi, like many other chemotherapeutics, have weaknesses limiting their efficacy *in vivo*: clearance, fast metabolism and poor specific accumulation in tumour leading to side effects [8].

In the field of anticancer strategies using chemotherapeutics with limited bioavailability, several types of drug delivery systems (DDS) have been proposed to protect the molecules from fast clearance, to circumvent solubility limitations and/or to selectively deliver compounds in tumour in order to decrease systemic toxicity. Typical examples of clinically used DDS are Doxil®, a liposome formulation containing doxorubicin, or Abraxane®, an albumin-paclitaxel conjugate. Only few examples of DDS applications designed for epigenetics have been reported that are mainly, in reality, for epigenetically repositioned compounds [9]. Developing novel strategies to improve novel HDACi benefits could thus come from delivery systems adapted to such compounds. However, the strategy can fail due to the limited compound solubility in the solvent conditions when preparing DDS micelles. Loading could be improved by converting HDAC inhibitors into more soluble compounds by new design. This re-development stage could be avoided by a simpler approach where current inhibitors are converted to soluble prodrugs [10] used in turn to prepared DDS. Alternatively, the prodrug could be covalently linked to the DDS to avoid leaks, a well-known problem with liposomes.

The choice of the releasing and DDS connection strategies is thus particularly important. If glucuronidation or conversion to esters were often used to prepared prodrugs they are not convenient strategies for HDAC inhibitor. Glucuronidation is interesting because glucuronidases are overexpressed in the tumour environment; however glucuronidation of HDAC inhibitors is a major metabolic pathway. On the other hand esterases are ubiquitous enzymes in humans and selective release from ester prodrugs at the tumour site cannot be achieved this way. Finally, epigenetic targets are mostly nuclear and this implies that the DDS or the prodrugs must preferably enter the cells and then release the compounds close to the nucleus. In the past decades, DDS strategy based on tumour cell internalization via endocytosis [11] and release at acidic pHs has appeared to be a convenient answer to these challenges. This strategy is also particularly interesting to avoid release of the compounds at physiological pHs during blood circulation. Polymer conjugates were investigated with a particular emphasis for pH-mediated release [12,13] through endocytosis. pH-Mediated release is also a practical solution avoiding complex prodrug syntheses, like those developed for glucuronidase strategies.

We applied the DDS strategy associated with a pH mediated release system to CI-994 (Tacedinaline). This HDACi is a member of the benzamide-related group, demonstrating interesting anti-tumor effects on cancer cells in culture. CI-994 inhibits preferentially the nuclear HDAC class I (HDAC1-3) [14] directly participating in the stimulation of TSG expression in cancer cell lines. CI-994 has higher half live than other HDAC inhibitors, as shown by [^{3}H] radiolabelled derivative [15], which is in part due to moderate protein binding *in vivo* allowing a histone deacetylation effect in a wider time range. Despite these long-ranging effects, the results obtained in clinic were disappointing [8]. Indeed, the principal dose limiting toxicity was thrombocytopenia and no evident anti-tumor effect was observed [8,16]. This demonstrates that stability is not the major weakness of this class of drugs and that systemic toxicity and probably diffusion in tumour tissues also constitute major barriers for clinical efficacy. Thus, this HDACi seemed to be a good candidate for vectorization strategy using DDS. We previously synthesized the acid-responsive prodrug **3** (Scheme 1) for CI-994, with a tetraethylenoxide chain to improve water solubility [17]. This novel releasing system was designed for cleavage at mildly acidic pH corresponding to the pH found in endosomes/lysosomes generated during the endocytosis-mediated internalization. This type of prodrug has demonstrated convenient stability at physiological pH and effective release at low acidic pH. This CI-994 prodrug has also shown good restoration of the initial HDAC inhibition, correlated with cancer cell death. In this work, it was thus envisioned to attach this prodrug to DDS able to enter cancer cells and protecting the prodrug from external metabolism. Exploiting endocytosis for DDS internalization allows for both DDS and the prodrug to be respectively degraded and cleaved when exposed to the acidic endosome/lysosome pathways. Several methods are available to connect prodrugs to DDS, a currently popular one being the bioconjugation based on the click chemistry concept [18–20] involving the reaction between alkyne and azide groups. These rationales were the basis for initial introduction of an alkyne group on the PEO-end chain of the prodrug system **3** to allow future grafting to DDS by click chemistry, implying that the DDS should bear azide groups. Within the several polymeric nanoparticles systems available [21] living Ring-Opening Metathesis Polymerization (ROMP) has recently emerged as an alternative method to produce therapeutic DDS and offers opportunities for well-defined spherical core–shell polymeric nanoparticles. We demonstrated that such biopolymers can be obtained from norbornenyl-PEO macromonomers adapted to the click chemistry reaction and that the final nanoparticles can natively enter cancer cells by endocytosis without any additional chemistry [22,23].

We hypothesized that the generic azido-norbornenyl-PEO macromonomer **5** (Scheme 1) involved in our ROMP-DDS synthesis could be made functional with our alkyne-bearing CI-994 acid-responsive prodrug **3** [17]. In this contribution we report our investigations in the synthesis of such pH responsive CI-994-bearing DDS and its physical and chemical characterization. Delivery of the HDACi in cells and restoration of HDAC inhibition was evaluated. Anti-tumor properties of our DDS on malignant pleural mesothelioma (MPM) and lung adenocarcinoma (ADCA) cancer cells, two forms of aggressive thoracic cancers with poor chemotherapeutic options, was studied in comparison with free CI-994 and bare DDS.

2. Results and discussion

2.1. Syntheses

The key macromonomer **6** (Scheme 1) was synthesized by azide-alkyne click chemistry from macromonomer **5** [23] and derivative **3** [17] best suited for CI-994 release at endosomal/lysosomal pH 5. Good yields in Huisgen cycloaddition required 2 equivalents of CuBr and the ligand PMDETA and 1.5 equivalent of the alkyne **3**. The formation of the macromonomer **6** was confirmed by ^{1}H NMR (Fig. 1). Protons signals for the prodrug part were assigned according to the ^{1}H NMR of the starting prodrug **3**, as no major shifts were observed after cycloaddition. The two key difference were the disappearance of the alkyne proton signal

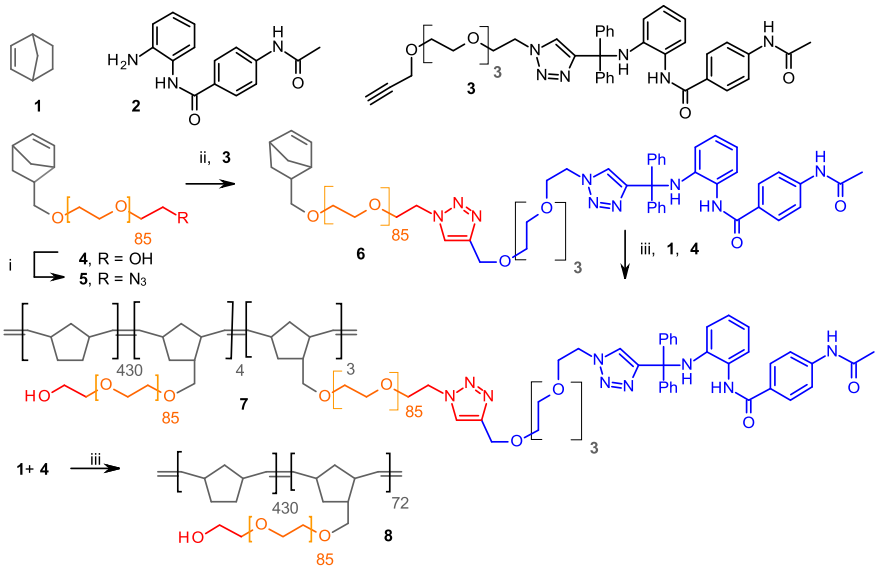

Scheme 1. (i) a – MsCl; b – NaN_3 (ii) CuBr (2eq.), PMDETA (2eq.), **3** (1.5 eq.) (iii) **4** (1% mol), **1** (98% mol) and **6** (1% mol), Grubbs I, CH_2Cl_2/EtOH 35/65 v/v, 20 °C, 24 h.

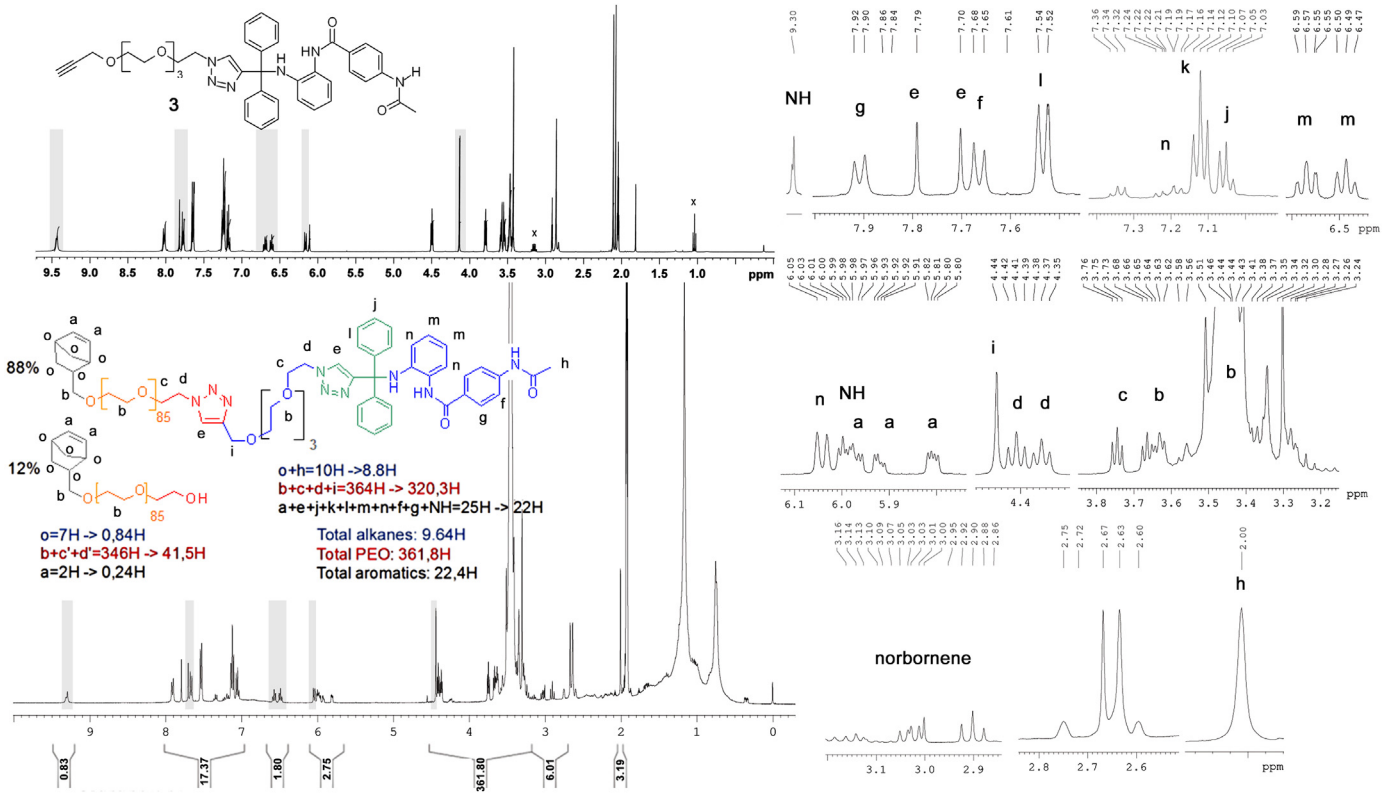

Fig. 1. Comparison of ^{1}H NMR of clickable prodrug **3** and macromonomer **6**. Some key hydrogen signals are greyed.

converted to the new triazole proton signal at 7.8 ppm and the shift of the methylene group of the terminal propargyl ether of prodrug **3** when clicked to the azidomacromonomer **5**. This methylene group shifted from 4.1 to 4.5 ppm. For the PEO-NB part, characteristic proton signals were observed: the NB double bond ($\delta = 5.8–6.2$ ppm, protons **a**), PEO chain ($\delta = 3.6–4.0$ ppm, protons **b**), and the new triazole ring signal ($\delta = 7.75$ and 7.8 ppm, proton **e**). Comparing the PEO protons **b** and NB protons **a** integration ratios before and after the functionalization, we could assume the conservation of the polymerizable part in the macromonomer **6**. Regarding the integration ratios for triazole ring proton **e** and the NB double bond protons **a** signals, a functionalization yield of about 88% could be calculated.

Grubbs I catalysed copolymerization of macromonomers **4** and **6** with NB **1** gave the copolymer **7** forming well defined spherical NPs in our dispersed media conditions with a hydrophobic polynorbornene core and a hydrophilic PEO shell. The composition of the latex was determined according to consumed starting

monomer and macromonomers with a reported method detailed in experimental section [23]. NB was polymerized to completion while overall macromonomer conversion (π) was about 90%. It is assumed than both macromonomers **4** and **6** were consumed at the same rate (we approximated that the ω-functionalization did not modify the reactivity of the macromonomers **4** and **6**).

The amount of prodrug per gram of polymer can be calculated according to the following formula:

$$\frac{n_{prodrug}}{g_{polym}} = \frac{F_{Prodrug} \times n_6 \times \pi}{\pi(m_6 + m_4) + m_1} = 49.6\ \mu mol/g$$

where $F_{Prodrug}$ is the functionalization yield of macromonomer **6** (0.88), n_6 is the amount of macromonomer **6** introduced for the NPs synthesis, π is the overall conversion of the macromonomers **4** and **6**, m_i is the weight of the compound **i** introduced for the synthesis of the NPs.

The polymer concentration can be estimated with the equation:

$$[polymer] = \frac{\pi(m_6 + m_4) + m_1}{V} = 43.0\ mg/mL$$

where V is the volume of the latex solution (12 mL).

Taking into account the amount of prodrug per gram of polymer and the polymer concentration the prodrug concentration can be evaluated to 2.13 mM.

The NPs **7** were then characterized by DLS (Fig. 2). The average size of the NPs in CH_2Cl_2/EtOH as solvents was 350 nm with a narrow dispersity (0.04). The amount of linked prodrug per NP ($n_{Prodrug/NP}$) can also be calculated by multiplying the number of prodrug per gram of polymer with the weight of an NP using the following equation [27]:

$$\frac{n_{Prodrug}}{NP} = n_{Prodrug/gpolym} \times V_{NP} \times \rho_{NP} \times N_A$$
$$= 6.7\ 10^8 \text{ active molecules per NP}$$

where V_{NP} is the volume of an NP ($V_{NP} = \pi D_{NP}^3/6$) (Fig. 2), ρ_{NP} is the density of the NPs approximated to equal to 1 g/mL, N_A is the Avogadro constant

The NPs were transferred in an aqueous solution of Trizma®base (10 mM) by successive evaporation and an ultrafiltration steps to give a final latex concentration of 6.9 mg/mL (prodrug concentration: 0.336 mM). The final particle size in aqueous solution was 320 nm. With non-functionalized NPs [23], the PEO shell expansion tends to increase the NP size in aqueous medium. Functionalized NPs **7** size decreased after their transfer in water due to the hydrophobic nature of the prodrug, which balance the PEO expansion. A final dilution was performed in order to obtain a polymer concentration of 1.72 mg/mL which corresponds to a prodrug concentration of $8.5 \cdot 10^{-2}$ mM for the biological purposes.

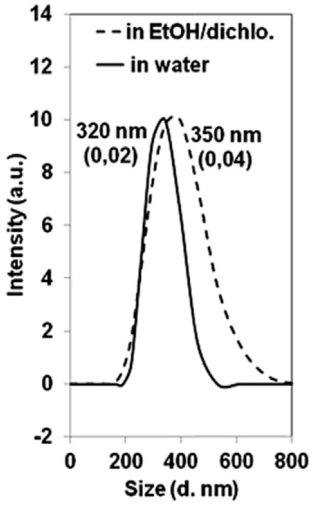

Fig. 2. Distribution of the NPs **7** size by intensity measure by DLS in the solvent mixture (EtOH/CH_2Cl_2) and in water.

NPs **7** should then be submitted to biological endocytosis-mediated internalization in cells to release the bioactive compound **2** upon acidification. Thus inhibitor **2** being covalently linked to NPs **7** by a pH responsive group, exposition to acidic vesicles like endosomes/lysosomes during endocytosis should give a functional release. This in turn will give diffusion of compound **2** in cells and restoration of HDAC inhibition. Unfunctional NPs **8** used as biological negative control was described previously [23].

2.2. HDACi release and activity in cells

To confirm the NPs internalization and HDAC release hypothesis, we used a bioluminescent resonance energy transfer (BRET) assay developed by some of us based on interactions between acetylated histones and BrD-containing proteins [28] (Fig. 3). The BRET response being obtained only if the compounds of interest are entering the cells to inhibiting HDACs, this assay can indicate both the cellular internalization of the nanoparticles and the release of the HDAC inhibitors of interest if the BRET signal is increased. Cells were treated in a dose dependent manner with CI-994 2 or NPs **7** during 16 h to monitor BRET signal induction. Free CI-994 induced a strong BRET at concentration below 25 μM that decreased for higher concentrations (Fig. 3A). In contrast, the BRET signal induced by NPs **7** was lower but maintained in relative higher amount even at higher equivalent CI-994 concentrations.

From these results of dose response experiments, BRET kinetics experiments were performed with four groups of MeT-5A cells (Fig. 3B) treated with 10 μM CI-994 and 1.72 mg/mL NPs **7** (85 μM CI-994) and the treatment stopped after 8 h, 24 h, 36 h and 48 h (respectively groups of cells 1–4). After 24 h treatment (group 2), HDAC inhibition effect for CI-994 was stabilized and then decreased after 36 h (group 3) while the effect of NPs **7** was increased all along the experiment (Fig. 3B). Fig. 3C indicates that the maximum BRET signal induction obtained with CI-994 and NPs **7** during the kinetic experiments were similar but not at the same time. The release kinetic obtained with NPs **7** is similar to the one obtained with the prodrug alone [17] demonstrating that the acido-sensitive release property of CI-994 is not altered in the DDS. These results showed that free CI-994 is able to rapidly enter cells compared to NPs **7** but with a limited activity over time, a result coherent with its half live (around 1 day) [8]. In contrast, NPs **7** effect is continuous over time suggesting that the internalization barrier and subsequent release are two events delaying the BRET signal induction.

2.3. Cancer cells killing properties of vectorised CI-994

When cancer cells are treated with HDAC inhibitor the expected biological effect is cell death induction mediated by stimulation of TSG. Thus the restored HDAC inhibition can be correlated with toxicity towards cancer cells. To verify this hypothesis, we used 3 lung ADCA and 3 MPM cell lines, representing 2 types of aggressive thoracic cancer cells. In Fig. 4, toxicity of NPs **7** was compared with free CI-994 against ADCA and MPM cell lines and unfunctional NPs **8** (Scheme 1) used as reference. No toxic effects of NPs **8** at 2 mg/mL were observed on the two types of cancer cell lines tested (Fig. 4). The decrease of ADCA cells viability (Fig. 4A) obtained with increasing doses of NPs **7** was similar to the effect of free CI-994

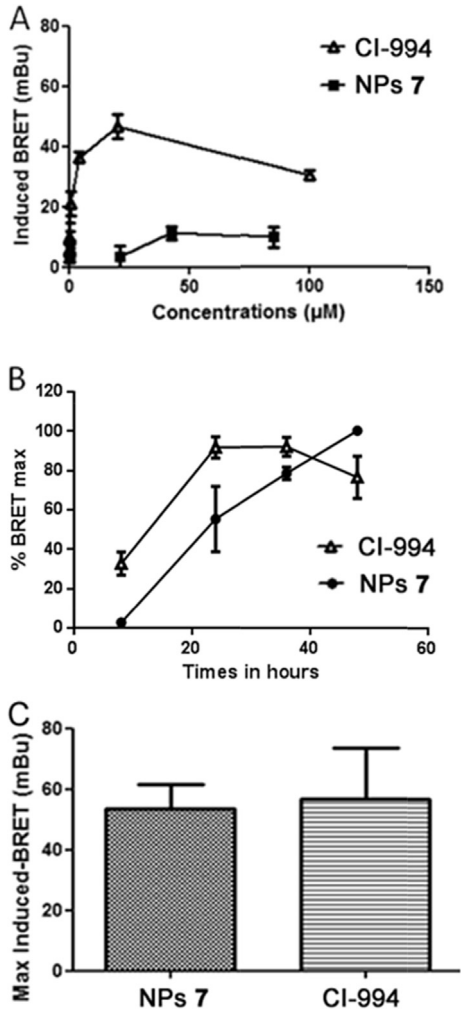

Fig. 3. Pharmacological characterization of NPs **7** using BRET in living cells. MeT-5A cells were transfected with phRluc-C1 BrD and pEYFP-C1 histone H3 expression vectors. A) Cells treated in a dose dependent manner with CI-994 **2** or NPs **7** during 16 h. B) Cells were treated during 8, 24, 36 or 48 h with 10 μM of CI-994 or 1.72 mg/mL of NPs **7** (85 μM of CI-994). Results were expressed as the percent of the maximal BRET signal obtained during the experiment. C) Graphic represents the maximal induced-BRET signal measured in kinetic experiment for each molecule independently of the time of treatment. Results are the means ± S.E.M of three independent experiments.

demonstrating that CI-994 activity was not altered by the grafting to the DDS. However, on MPM cells (Fig. 4B), toxicity of NPs **7** was lower than the one of free CI-994. In these experiments, the

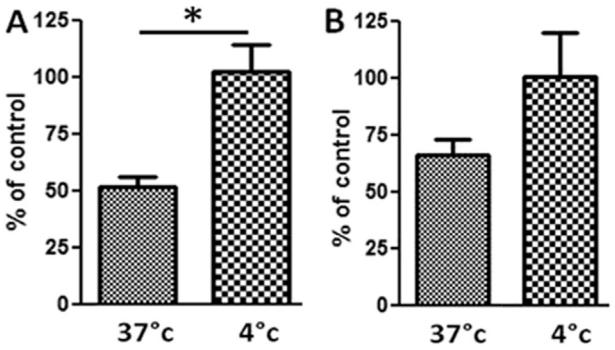

Fig. 5. Temperature effect on cells viability after treatment with NPs **7** of A) Groups of lung ADCA and B) MPM cells with 1.72 mg/mL NPs **7** (85 μM CI-994) for 8 h at 4 °C or 37 °C. Then, media were changed and cells were incubated at 37 °C for additional 64 h. Cell viability was expressed as the percent of control. Results are the means ± S.E.M of the results obtained on three different lung ADCA and MPM cell lines. *$p < 0.05$.

decreased viability induced by NPs **7** can be exclusively attributed to CI-994 release regarding the polymer concentration. Indeed, NPs **7** were used at a polymer concentration of 1.72 mg/mL which is lower than the nontoxic NPs **8** concentration tested (2 mg/mL).

The requirement of an active internalization of NPs **7** to obtain toxicity was demonstrated by viability experiments performed by treating ADCA and MPM cells with NPs **7** or CI-994. Two groups of ADCA and MPM cells were treated at 4 °C to block active internalization mechanisms and two other groups of ADCA and MPM cells were treated at 37 °C as control (Fig. 5). Effect of NPs **7** on viability was completely abolished in cells treated at 4 °C compared to those treated at 37 °C for the two types of cancer cell lines tested. This result demonstrated that NPs **7** need an active mechanism for internalization, likely clathrin-independent receptor-mediated macropinocytosis as we previously described [22], and excluded an eventual spontaneous release of CI-994 in the medium.

Apoptosis of cancer cells is increased upon HDACi treatments in vitro. Treatments of ADCA and MPM cell lines with 1.72 mg/mL NPs **7** (85 μM CI-994) for 48 h (Fig. 6) showed effective apoptosis revealed by Annexin-V labelling. As observed for viability, lung ADCA cells seemed to be more sensitive to NPs **7**-induced apoptosis than MPM cells. The difference of sensitivity of the two types of cancer cell lines tested towards NPs **7** can be explained by the low endocytic activity of mesothelial cells [29] confirmed by our previous work [22] in which we showed that MPM cells displayed a weak NPs endocytic capacity compared to lung ADCA cells. This difference of properties results here, in a lower level of intracellular CI-994 and then to a lower toxicity of NPs **7** on MPM cells compared to lung ADCA cells.

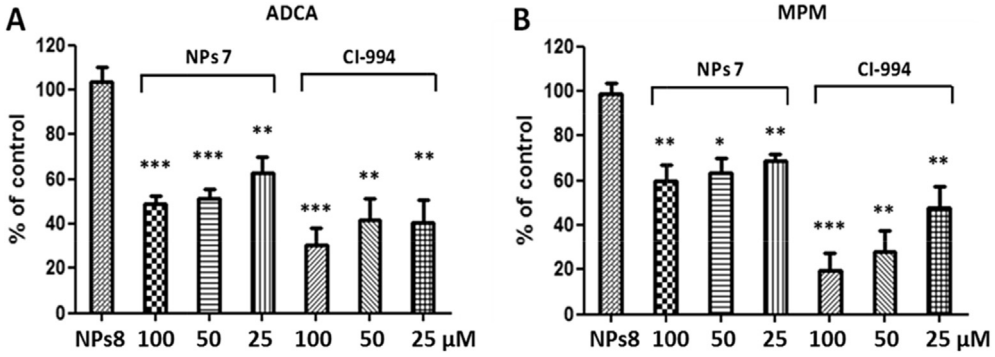

Fig. 4. Effect of CI-994, NPs **7** and **8** on A) lung ADCA and B) MPM cells viability. Lung ADCA and MPM cells were treated with 2 mg/mL of NPs **8** and increasing concentrations of CI-994 or NPs **7** for 72 h. Results are the means ± S.E.M of the results obtained on three different lung ADCA and MPM cell lines. *$p < 0.05$; **$p < 0.01$; ***$p < 0.001$.

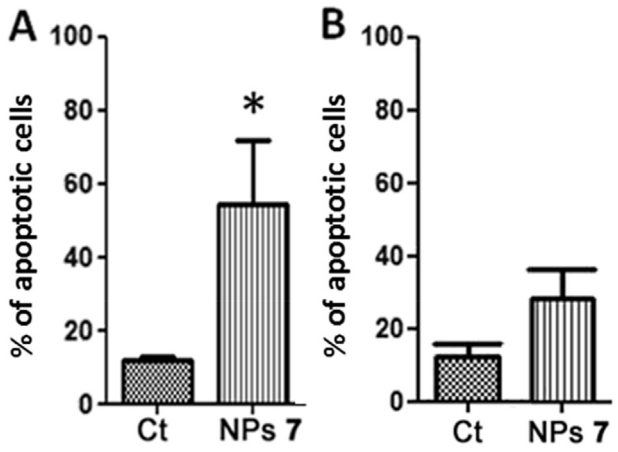

Fig. 6. Apoptosis of A) ADCA and B) MPM cell lines treated with 1.72 mg/mL NPs **7** (85 μM CI-994) for 48 h. Apoptosis was evaluated using Annexin-V-FITC labeling and flow cytometry analysis. Results are the means ± S.E.M of the results obtained on three different lung ADCA and MPM cell lines. $^{*}p < 0.05$.

3. Conclusions

We described an easy and effective method to introduce acid-responsive HDACi prodrug on azido-PEO-NB macromonomers by click chemistry as an entry toward nanoparticles prepared by ROMP. This synthetic method should allow accessing multifunctional particles by the click chemistry concept [18] if more specific cell targeting or internalization is required by adding dedicated functions on the starting azido-macromonomer, like RGD substrate of integrins or cell penetrating peptides. The NB and PEO parts of the macromonomer allow for the formation of well-defined core (NB)-shell (PEO) spherical nanoparticles with homogenous 300 nm sizes, all parameters not modified by the introduction of the prodrug component. The positioning of the PEO part at the surface of the nanoparticles introduce native stealth properties that may also not be modified by the introduction of the prodrug component present in only 1% mole relative to the NB part. We have demonstrated that HDACi vectorization is a viable alternative with such NPs entering cells by an active mechanism without additional chemistry. The release of the HDAC inhibitor in cells was validated by our BRET assay and this release was correlated with cell viability and apoptosis. Several other classes of compounds are currently studied as epigenetic target inhibitors in various diseases (inhibitors of histone methylation and demethylation, DNA methyl transferases, protein arginine methyl transferases, sirtuins). This work opens the way for future delivery of these emerging chemotherapeutics. In a previous study [22], we also demonstrated that a fluorescent version of this DDS can accumulate mainly in tumour *in vivo* by exploiting the enhanced permeability and retention effect (EPR) described in tumour tissues [30], being thus a promising carrier to circumvent clearance and metabolism of chemotherapeutics and to improve the clinical benefit of HDACi in particular for solid tumour therapy by decreasing side effects.

4. Materials and methods

4.1. General

Ethanol (96%, purissium grade pur, Xilab), dichloromethane (96%, purissium grade pur, Xilab) and dimethyl formamide (DMF, 99.8%, Panreac) were degassed before use. The solvents were degassed according to the freeze–pump–thaw procedure. Tetrahydrofuran (THF, J.T. Baker) anhydrous diethyl ether (J.T. Baker), *N*,*N*,*N*′,*N*″,*N*″-pentamethyldiethylenetriamine (PMDETA, 99%, Aldrich), Na_2SO_4 (99%, Alfa Aesar), norbornene (99% GC, Aldrich), Grubbs first generation catalyst $Cl_2(PCy_3)_2Ru$ = CHPh (Aldrich, stored in a glovebox under Argon atmosphere), dodecane (99%, Aldrich), triethylamine (TEA, 99%, Acros Organics), ethyl vinyl ether (99% stab. with ca. 0.1% *N*,*N*-diethylalanine, Alfa Aesar), Trizma®-base (99.9%, Aldrich) were used without further purification. CuBr (98%, Aldrich) was purified in acetic acid and stored under inert atmosphere (glovebox). Macromonomers 4 (M_n = 3910 g mol^{-1}) and 5 (M_n = 3930 g mol^{-1}) were prepared according to procedures described in the literature [23,24]. The polymerization reaction was carried out at room temperature under inert atmosphere (glovebox).

4.2. Syntheses

4.2.1. Prodrug-functionalized macromonomer 6 (Scheme 1, Fig. 1)

Alkyne **3** (394 mg, 0.55 mmol), macromonomer **5** (1.445 g, M_n = 3930 g mol^{-1}, 0.37 mmol), and PMDETA (153 μL, 0.74 mmol) were dissolved in DMF (15 mL) and the mixture degassed according to the freeze–pump–thaw procedure. CuBr (105 mg, 0.74 mmol) was added under inert atmosphere (glovebox). The mixture was stirred during 4 days under argon at room temperature. CH_2Cl_2 (90 mL) was added to the reaction mixture and the solution washed with H_2O (10 × 60 mL), dried (Na_2SO_4), filtered and the solvents evaporated. The crude macromonomer **6** was dissolved in THF (50 mL) and precipitated in diethyl ether (250 mL), filtered, dried under vacuum and finally lyophilized in dioxane. The macromonomer **6** was stored under argon before use. ^{1}H NMR in Acetone D6: (δ in ppm) 9.31 + 9.29 (s, 2H), 7.91 (d, J = 8.5 Hz, 2H); 7.79 (s, 1H), 7.70 (s, 1H), 7.66 (d, J = 8.6 Hz, 2H), 7.53 (d, J = 7.6 Hz, 4H), 7.34–7.05 (m, 9H), 6.57 (dt, J = 1.2, 11.6 Hz, 1H), 6.49 (t, J = 7.6 Hz, 1H), 6.04 (d, J = 8.4 Hz, 1H), 6.00 (st, 1H), 5.88 (m, 2H), 4.44 (s, 2H), 4.41 (t, J = 4.8 Hz, 2H); 4.37 (t, J = 5.2 Hz, 2H), 3.75 (t, J = 5.2 Hz, 2H), 3.67 (t, J = 4.8 Hz, 2H), 3.63 (m, 2H); 3.45 (s, 355H), 3.2–2.98 (m, H cycles NB), 2.90 (t, J = 9.2 Hz, 2H), 2.04 (s; 3H). Functionalization yield of macromonomer **6** ($F_{prodrug}$) was 88%; Size exclusion chromatography (SEC) in THF: (RI) M_n = 3390 g mol^{-1} (styrene eq.); Polydispersity index (PDI) = 1.09.

4.2.2. ^{1}H NMR based calculation of macromonomer **6** molecular weight M_n

^{1}H NMR studies were completed with a Bruker spectrometer 400 MHz, in $CDCl_3$ or in acetone D6 at 25 °C. Dynamic light scattering (DLS) measurements were performed using a MALVERN zetasizer Nano ZS equipped with He–Ne laser (4 mW and 633 nm). Before measurements, latexes were diluted about 800 times to minimize multiple scatterings caused by high concentration. The scattering angle used was 173°. The macromonomer **6** can be view as a mixture of unfunctionalized (12%) and functionalized (88%) macromonomers. The number average molecular weight (M_{nNMR}) of **6** can be calculated by using the ^{1}H NMR spectra following the equation:

$$M_{nNMR} = 0.88 \times (M_{NB} + M_{EO} \times DP_n + M_{Prodrug}) + 0.12 \times (M_{NB} + M_{EO} \times DP_n + M_{EtOH})$$

$$M_{nNMR} = 0.88 \times (123 + (44 \times 85) + 787) + 0.12 \times (123 + (44 \times 85) + 45) = 4561 \text{ g mol}^{-1}$$

where M_{NB} is the molecular weight of the PEO α-functionalization, M_{EO} is the molecular weight of an ethylene oxide unit, $M_{Prodrug}$ is the molecular weight of ω-end group of macromonomer **6**, M_{EtOH} is the molecular weight of ω-end group of unfunctionalized macromonomer **4**. DP_n is the number average polymerization degree

DPn = (IPEO/4)/(INB/2), IPEO is the integration of the protons signal of the PEO chain, INB, is the integration of the signals of the ethylenic protons of the norbornenyl entity.

4.2.3. Synthesis of NPs **7** (Scheme 1, Fig. 2)

Grubbs first generation complex (10 mg, 1.2 × 10^{-5} mol) was dissolved in CH_2Cl_2/EtOH (5 mL, 50/50% v/v). Norbornene (387 mg, 4.1 × 10^{-3} mol), macromonomers **4** (125 mg, 3.2 × 10^{-5} mol) and **6** (190 mg, 4.2 × 10^{-5} mol) were first dissolved in CH_2Cl_2/EtOH (7 mL, 35/65% v/v) and added to the catalyst solution. NEt_3 (0.1 mL) was added to maintain the pH solution higher than 7. The mixture was stirred during 24 h. At the end of polymerization ruthenium end-capped chains were deactivated by addition of 0.3 mL of ethyl vinyl ether. The conversion of macromonomers was determined by SEC with dodecane as internal standard (SEC retention times: $t^{SEC}_{macromonomers}$ = 18.75 min; $t^{SEC}_{dodecane}$ = 31.70 min). SEC equipment consisted of a JASCO HPLC pump type 880-PU, TOSOHAAS TSK gel columns, a Varian refractive index detector, and a JASCO 875 UV–vis absorption detector, with THF as the mobile phase and the calibration curve was performed using polystyrene standards. The conversion of NB was determined by gas chromatography with dodecane as internal standard (GC retention times: t^{GC}_{Nb} = 1.77 min = 1.77 min; $t^{GC}_{dodecane}$ = 8.55 min). Gas chromatography measurements were performed with a Varian 3900 apparatus having a Factor Four Capillary Column VF-1ms 15 M × 0.25 MM ID DF = 0.25 (injector: T = 250 °C; oven: Initial temperature: 50 °C during 2 min followed by a temperature rate of 10 °C/min until 250 °C; detector: T = 300 °C).

4.3. Biology

4.3.1. Cell culture

The pleural mesothelial cell line, MeT-5A, and the lung adenocarcinoma cell line, A549, were obtained from American Type Culture Collection (ATCC). The mesothelioma cell lines Meso13, Meso34 and Meso56 and the lung adenocarcinoma cell lines ADCA 153 and ADCA 72 were established from the pleural fluids of patients [25]. All cell lines were maintained in RPMI medium (Invitrogen) supplemented with 2 mM L-glutamine, 100 IU/mL penicillin, 0.1 mg/mL streptomycin and 10% heat inactivated foetal calf serum (FCS) (Eurobio).

4.3.2. BRET experiments (Fig. 3)

The principle was to transfect MeT-5A cells with two cDNA, one coding for bromodomain (BrD) fused with a luciferase and one coding for histone H3 fused with yellow fluorescent protein, leading to the expression of the two recombinant proteins in cell nucleus. HDAC inhibition resulted in higher levels of acetylated histones, increased interactions of the two tagged proteins and in turn increased BRET signal. MeT-5A cells were seeded at a density of 1.5 × 10^5 cells per 35 mm dish. Transient transfections were performed one day later using Attractene (Qiagen), according to the manufacturer's protocol. For BRET experiments, MeT-5A cells were transfected with 0.6 μg Rluc-Brd cDNA and 1 μg YFP-fused histone H3 cDNA [26]. One day after transfection, cells were transferred into 96-well microplates (microplate 96 well, white, Berthold Technologies) at a density of 3 × 10^4 cells per dish. All BRET measurements were performed the following day at room temperature using the Mithras LB 940 microplate analyzer (Berthold Technologies). Cells were pre-incubated for 15 min in PBS in the presence of 2.5 μM coelenterazine (Interchim), following which light-emission acquisition at 485 and 530 nm was carried out. Plates were measured five times. The BRET signal was expressed in milliBRET units (mBu). The BRET unit has been defined previously as the ratio 530/485 nm obtained when the two partners are present, corrected by the ratio 530/485 nm obtained under the same experimental conditions, when only the partner fused to *Renilla* luciferase is present in the assay.

4.3.3. Determination of cell viability (Fig. 4)

Cell growth was monitored using Uptiblue reagent (Interchim). Reduction of this compound by the cell results in the formation of a fluorescent compound quantified by measuring fluorescence at 595 nm after excitation at 532 nm using a Typhoon apparatus (GE Healthcare). Cells were seeded in 96-well plates at a density of 5 × 10^3 cells/well in culture medium. Twenty-four hours later, compounds solutions or nanoparticles were added for 72 h. Uptiblue (5%, v/v) was then added to the culture medium for 2 h at 37 °C. Fluorescence was quantified by measuring emission at 595 nm after excitation at 532 nm using a Typhoon apparatus.

4.3.4. Evaluation of temperature on NPs **7** toxicity (Fig. 5)

Cells were seeded in 96-well plates at a density of 5 × 10^3 cells/well in culture medium. Twenty-four hours later, two groups of cells were treated with 1.72 mg/mL NPs **7** (85 μM CI-994) for 8 h at 4 °C (group 1) or 37 °C (group 2). Then, media were changed and cells were incubated at 37 °C for additional 64 h. Cell viability was evaluated using Uptiblue cell counting reagent as described above.

4.3.5. Detection of apoptosis (Fig. 6)

Apoptosis was quantified using the Annexin V-fluorescein-isothiocyanate (FITC) (*Becton Dickinson*), which labels phosphatidylserine externalized in the early phases of apoptosis. Cells were seeded at a density of 1 × 10^5 per well of 6-wells plates and treated with NPs **7** 1.72 mg/mL (85 μM CI-994). After 48 h of culture, floating and adherent cells were combined, washed twice with cold PBS, resuspended in 100 μL of annexin binding buffer (10 mM Hepes, 140 mM NaCl, 2.5 mM $CaCl_2$, pH 7.4), incubated for 15 min at room temperature with 2.5 μL of Annexin V-FITC and analysed by flow cytometry (FACSCalibur; Becton Dickinson). Ten thousand events were collected and analysed with the FACS Flowjo Software.

4.3.6. Statistical analysis

Statistical analyses were performed using GraphPad prism, (Prism 5, Windows). Statistical comparisons were made using an unpaired t-test.

Author contributions

FEB, RD and PB synthetized and characterized CI-994 prodrug. FC and LP produced and characterized nanoparticles. ID, FG and DP carried out all cellular experiments and interpreted the data. VH, PB, MG and CB coordinated this study, designed the experiments, interpreted the data and wrote the manuscript.

Conflict of interest

Authors declare no conflict of interest.

Acknowledgments

This work was supported by Agence Nationale de la Recherche (ANR) for RD, FG and FC grants (ANR-08-PCVI-030), Région Poitou-Charentes for FEB grant, Centre National de la Recherche Scientifique (CNRS), the Ligue National Contre la Cancer for ID grant, the Ligue Contre le Cancer: committees of Morbihan, Sarthe, Vendée et Loire-Atlantique, Poitou-Charentes, ARSMESO44, Nantes University Hospital, and COST action TD0905.

Appendix A. Supplementary data

Supplementary data related to this article can be found at http://dx.doi.org/10.1016/j.ejmech.2015.03.037.

References

[1] P.A. Jones, S.B. Baylin, Nat. Rev. Genet. 3 (2002) 415.
[2] D. Dhanak, ACS Med, Chem. Lett. 3 (2012) 521.
[3] C.H. Arrowsmith, C. Bountra, P.V. Fish, K. Lee, M. Schapira, Nat. Rev. Drug Discovery 11 (2012) 384.
[4] M.A. Glozak, E. Seto, Oncogene 26 (2007) 5420.
[5] S.S. Nair, R. Kumar, Mol. Oncol. 6 (2012) 611.
[6] P. Bertrand, Eur. J. Med. Chem. 45 (2010) 2095.
[7] A.A. Lane, B.A. Chabner, J. Clin. Oncol. 27 (2009) 5459.
[8] N. Martinet, P. Bertrand, Cancer Manage. Res. 3 (2011) 117.
[9] F. El Bahhaj, F.J. Dekker, N. Martinet, P. Bertrand, Drug Discovery Today 19 (2014) 1337.
[10] Y. Ishii, Y. Hattori, T. Yamada, S. Uesato, Y. Maitani, Y. Nagaoka, Eur. J. Med. Chem. 44 (2009) 4603.
[11] G. Scita, P.P. Di Fiore, Nature 463 (2010) 464.
[12] M. Hruby, C. Konak, K. Ulbrich, J. Control. Release 103 (2005) 137.
[13] L.M. Kaminskas, B.D. Kelly, V.M. McLeod, G. Sberna, D.J. Owen, B.J. Boyd, C.J.H. Porter, J. Control. Release 152 (2011) 241.
[14] N. Khan, M. Jeffers, S. Kumar, C. Hackett, F. Boldog, N. Khramtsov, X. Qian, E. Mills, S.C. Berghs, N. Carey, P.W. Finn, L.S. Collins, A. Tumber, J.W. Ritchie, P.B. Jensen, H.S. Lichenstein, M. Sehested, Biochem. J. 409 (2008) 581.
[15] Y. Wang, Y.L. Zhang, K. Hennig, J.P. Gale, Y. Hong, A. Cha, M. Riley, F. Wagner, S.J. Haggarty, E. Holson, J. Hooker, Epigenetics 8 (2013) 756.
[16] S. Prakash, B.J. Foster, M. Meyer, A. Wozniak, L.K. Heilbrun, L. Flaherty, M. Zalupski, L. Radulovic, M. Valdivieso, P.M. LoRusso, Invest. New. Drugs 19 (2001) 1.
[17] R. Delatouche, I. Denis, M. Grinda, F. el Bahhaj, E. Baucher, F. Collette, V. Héroguez, M. Grégoire, C. Blanquart, P. Bertrand, Eur. J. Pharm. Biopharm. 85 (2013) 862.
[18] C.D. Hein, X.M. Liu, D. Wang, Pharm. Res. 25 (2008) 2216.
[19] R. Huisgen, Angew. Chem. Int. Ed. Engl. 2 (1963) 565.
[20] H.C. Kold, M.G. Fin, K.B. Sharpless, Angew. Chem. Int. Ed. Engl. 40 (2001) 2004.
[21] A. Nori, J. Kopecek, Adv. Drug Deliv. Rev. 57 (2005) 609.
[22] F. Gueugnon, I. Denis, D. Pouliquen, F. Collette, R. Delatouche, V. Héroguez, M. Gregoire, P. Bertrand, C. Blanquart, Biomacromolecules 14 (2013) 2396.
[23] F. Collette, R. Delatouche, C. Blanquart, F. Gueugnon, M. Gregoire, P. Bertrand, V. Héroguez, J. Polym. Sci. Part A 51 (2012) 176.
[24] V. Héroguez, S. Breunig, Y. Gnanou, M. Fontanille, Macromolecules 29 (1996) 4459.
[25] F. Gueugnon, S. Leclercq, C. Blanquart, C. Sagan, L. Cellerin, M. Padieu, C. Perigaud, A. Scherpereel, M. Gregoire, Am. J. Pathol. 178 (2011) 1033.
[26] C. Blanquart, M. Francois, C. Charrier, P. Bertrand, M. Gregoire, Curr. Cancer Drug Targets 11 (2011) 919.
[27] L. Pichavant, G. Amador, C. Jacqueline, B. Brouillaud, V. Héroguez, M.-C. Durrieu, J. Control. Release 162 (2012) 373.
[28] D.S. Hewings, T.P.C. Rooney, L.E. Jennings, D.A. Hay, C.J. Schofield, P.E. Brennan, S. Knapp, S.J. Conway, J. Med. Chem. 55 (2012) 9393.
[29] S.E. Mutsaers, J. Biochem. Cell. Biol. 36 (2004) 9.
[30] H. Maeda, Bioconjugate Chem. 21 (2010) 797.